Available online at www.sciencedirect.com
ScienceDirect
Journal of Power Sources 184 (2008) 695–700
JOURNAL OF POWER SOURCES
www.elsevier.com/locate/jpowsour

Short communication

Layer-by-layer self-assembly of manganese oxide nanosheets/polyethylenimine multilayer films as electrodes for supercapacitors

Xiong Zhang, Wensheng Yang *, David G. Evans

State Key Laboratory of Chemical Resource Engineering, Beijing University of Chemical Technology, Beijing 100029, China

Received 21 November 2007; received in revised form 20 December 2007; accepted 8 January 2008
Available online 18 January 2008

Abstract

Multilayer thin films of manganese oxide nanosheets (MNSs) and polyethylenimine (PEI) polyelectrolyte have been fabricated onto various substrates via layer-by-layer self-assembly technique. UV–vis absorption spectra showed that the absorbance values at the characteristic wavelength of the multilayer films increased almost linearly with the number of PEI/MNS bilayers. Field emission scanning electron microscope (FESEM) images indicated that the surface of the multilayer film was rather smooth and dense. The electrochemical performances of $(PEI/MNS)_n$ films on indium–tin oxide (ITO)-coated glass substrates were investigated by cyclic voltammetry and constant current charge–discharge test from 0 to 0.9 V in a 2 M KCl aqueous solution. The multilayer films showed excellent electrochemical activity, high reversibility and high power density. A specific capacitance value of 288 F g^{-1} was obtained at a current density of 1.25 A g^{-1} for $(PEI/MNS)_{10}$ film in 2 M KCl aqueous solution. The specific capacitance decreased 9.5% of initial capacity over 1000 cycles at a high current density of 2.5 A g^{-1}. These good electrochemical properties could be attributed to the special microstructure of the electrode.

Keywords: Manganese oxide nanosheets; Polyethylenimine polyelectrolyte; Layer-by-layer self-assembly; Supercapacitor

1. Introduction

Supercapacitors (also called electrochemical capacitors) are currently receiving great attention for their use as energy-storage devices that possess high power density, excellent pulse charge–discharge property and very long cycle life [1–3]. Traditionally, ruthenium oxides are the promising electrode materials for supercapacitors due to their high specific capacitance up to 720 F g^{-1} and excellent cyclability [4]. However, ruthenium oxides are expensive and toxic to environment.

Manganese oxides provide a lower cost, lower toxicity replacement for ruthenium oxides in supercapacitor applications. Manganese oxide thin film electrodes have been prepared by various synthesis methods, such as sol–gel dip- or drop-coating [5–7], electrochemical deposition [8–12], electrostatic spray deposition [13,14] and physical vapor deposition followed by electrochemical oxidation [15–17]. Pang et al. [5] investigated the electrochemical properties of sol–gel-derived MnO_2 thin films (~1 μg cm^{-2}), which exhibited a specific capacitance as high as 698 F g^{-1} after annealing at 300 °C for 1 h. However, the specific capacitance decreased with increasing film thickness due to the poor electrical conductivity of MnO_2. Broughton and Brett [15] reported a specific capacitance of 700 F g^{-1} in MnO_2 thin films (25–75 μg cm^{-2}) prepared by anodic oxidation of sputtered Mn films. The high specific capacitance obtained at a slow charging current decreased fast with increasing current or sweep rate in voltage. Nagarajan et al. [10] prepared manganese oxide films by polymer-assisted cathodic electrosynthesis from $MnCl_2$ and polyethylenimine solution in a mixed ethanol–water solvent. A specific capacitance of 445 F g^{-1} was obtained after the film annealing at 300 °C for 1 h. The use of polyethylenimine as an additive enabled the formation of adherent films, which exhibited enhanced resistance to cracking during drying.

Recently, layer-by-layer (LBL) adsorption technique has become one of the most promising new methods for thin film fabrication [18–20]. It is characterized as being relatively sim-

* Corresponding author. Tel.: +86 10 64435271; fax: +86 10 64425385.
E-mail address: yangws@mail.buct.edu.cn (W. Yang).

0378-7753/$ – see front matter © 2008 Elsevier B.V. All rights reserved.
doi:10.1016/j.jpowsour.2008.01.021

ple, inexpensive, and less energy consumption. In addition, it is easy to control the composition and thickness of the film. The inorganic nanosheets with thickness at nanoscale can be used as building blocks in the fabrication of thin film by LBL technique. The nanosheets have showed an increased diffusion-limited capacitance due to the more open framework compared to bulk materials [21]. We recently reported that Co–Al layered double hydroxides nanosheets may be a candidate electrode material for supercapacitor [22]. According to our knowledge, the supercapacitive behavior of manganese oxide nanosheets (MNS) thin film fabricated by LBL technique has never been studied before.

We report here for the first time to fabricate multilayer thin films of MNS with polyethylenimine (PEI) polyelectrolyte. The resulting films were characterized by atomic force microscopy (AFM), UV–vis absorption spectra, X-ray photoelectron spectra (XPS), and field emission scanning electron microscope (FESEM). We also studied the pseudocapacitive behaviors of these films in a neutral aqueous electrolyte by cyclic voltammetry and constant current charge–discharge test.

2. Experimental

2.1. Thin film preparation

The colloidal suspension of MNS was prepared by the method described in the literature [23]. A mixed solution of 0.6 M NaOH and 2 M H_2O_2 was quickly poured into a 0.3 M $Mn(NO_3)_2$ solution and stirred for 30 min. The precipitate was subjected to hydrothermal treatment at 150 °C for 16 h in a 2 M NaOH solution. The sodium birnessite obtained was acid treated with a 1 M HNO_3 solution for 3 days at room temperature, washed with water, and dried at 70 °C, which was designated as H-Birnessite. H-Birnessite (2 g) was treated in a 0.16 M aqueous solution of tetramethylammonium hydroxide (200 ml) for 7 days at 25 °C. After soaking, the suspension was centrifuged at a speed of 10,000 rpm for 20 min to obtain the MNS colloid.

In a typical process, substrates, such as Si wafers and quartz glass slides, were cleaned by first placing them in a hot H_2SO_4/H_2O_2 (7:3 in volume ratio) bath for about 1 h and then in a $H_2O/H_2O_2/NH_3$ (5:1:1 in volume ratio) bath at 40 °C for 30 min. The substrates were extensively rinsed with twice-distilled water after each cleaning step. Indium–tin oxide (ITO)-coated glass substrates were cleaned by sonication in acetone and washed with ethanol and twice-distilled water. The substrates were precoated with PEI by immersion in an aqueous solution of PEI (2.5 g dm^{-3}, pH 9) for 20 min. The PEI-primed substrates were then immersed in a colloidal suspension (0.2 g dm^{-3}, pH 9) of MNS for 20 min, followed by thorough washing with twice-distilled water. These operations were repeated n times to obtain multilayer films of $(PEI/MNS)_n$. The resulting films were dried with N_2 gas flow at room temperature.

2.2. Characterization

The surface topography of the film was examined using a NT-MDT Model-STM Solver P47 atomic force microscopy (AFM) in contact mode. UV–vis absorption spectra of the films were measured by a Shimadzu UV-2501PC spectrometer. FESEM images were taken from a Hitachi S4700 SEM. X-ray photoelectron spectroscopy (XPS) measurements were performed using a Thermo VG ESCALAB 250 instrument equipped with a monochromatic Al Kα X-ray source (1486.6 eV) at a constant analyzer pass energy of 20.0 eV. The binding energy scale was calibrated with respected to the C 1s (284.6 eV) signal. Curve fitting was made by a mixture of Gaussian and Lorenzian functions, while background subtraction was done according to the Shirley method.

2.3. Electrochemical measurements

The electrochemical cell used in this study was a three-electrode system. The $(PEI/MNS)_n$ thin film deposited on the ITO substrate (the geometric area of 2 cm^2) was used as the working electrode, a Pt sheet and a standard calomel electrode (SCE) were employed as the counter and reference electrodes, respectively. The mass of deposited manganese oxide thin film on ITO substrate was determined by dissolving the film in an H_2O_2/HNO_3 mixture and using inductively coupled plasma-atomic emission spectroscopy (ICP-AES) (Shimadzu ICPS-7500). Based on the measured concentration of Mn per unit volume, the total mass of deposited manganese oxides of the electrode was calculated using the formula weight of stoichiometric MnO_2 of 97 g mol^{-1}. Cyclic voltammetry (CV) scans were recorded from 0 to 0.9 V (vs. SCE) in a 2 M KCl aqueous solution by using a ZAHNER IM6e electrochemical workstation. Galvanostatic charge/discharge tests were evaluated with an Arbin MSTAT4+ multichannel galvanostat/potentiostat in the potential range of 0–0.9 V (vs. SCE).

3. Results and discussion

Fig. 1 shows the topographic image of the deposited layer of MNS on Si wafer. The lateral dimensions of MNS obtained by

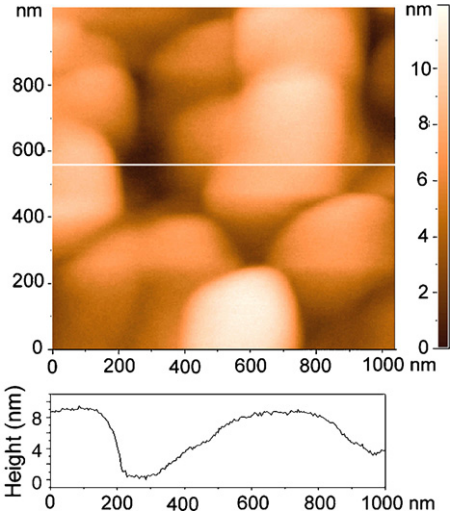

Fig. 1. AFM image with height profile along the white line of MNS deposited on PEI precoated Si wafer.

AFM observation are about 300 nm and the thicknesses are about 8 nm. Considering the thickness of manganese oxide lattice layers (0.45 nm) [23], one MNS should contain several inorganic lattice layers.

The MNS exhibit a broad adsorption band centered at around 320 nm, corresponding to a band gap of 2.37 eV. This spectral feature differs remarkably from that of the layered manganese oxide powder whose UV–vis spectrum reveals an almost constant and featureless absorption in the range of 200–800 nm [24]. The spectral change is due to the disassembly of bulk crystals into nanosheets with a nanometer thickness. The subsequent growth of self-assembled manganese oxide thin films can be monitored by UV–vis spectra measured immediately after each deposition cycle as shown in Fig. 2. The nearly linear increment of absorbance at 320 nm is observed, indicating that PEI polyelectrolyte and MNS are uniformly deposited by the LBL technique.

XPS data provide evidence for the incorporation of PEI polyelectrolyte and MNS in multilayer films. The XPS spectrum of $(PEI/MNS)_{10}$ film shows the main peaks in the regions of Mn 2s, 2p, 3s, 3p, O 1s, N 1s, and C 1s, as shown in Fig. 3a.

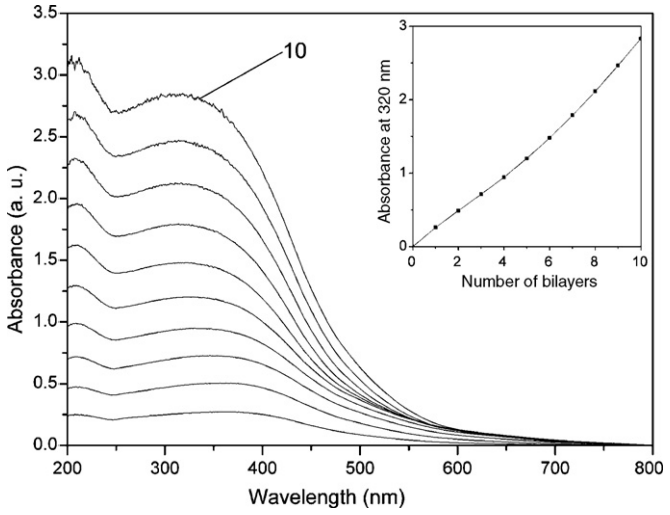

Fig. 2. UV–vis absorption spectra of multilayer films of $(PEI/MNS)_n$ prepared on quartz glass substrates. The insert shows the dependence of absorbance at 320 nm as a function of deposition cycles.

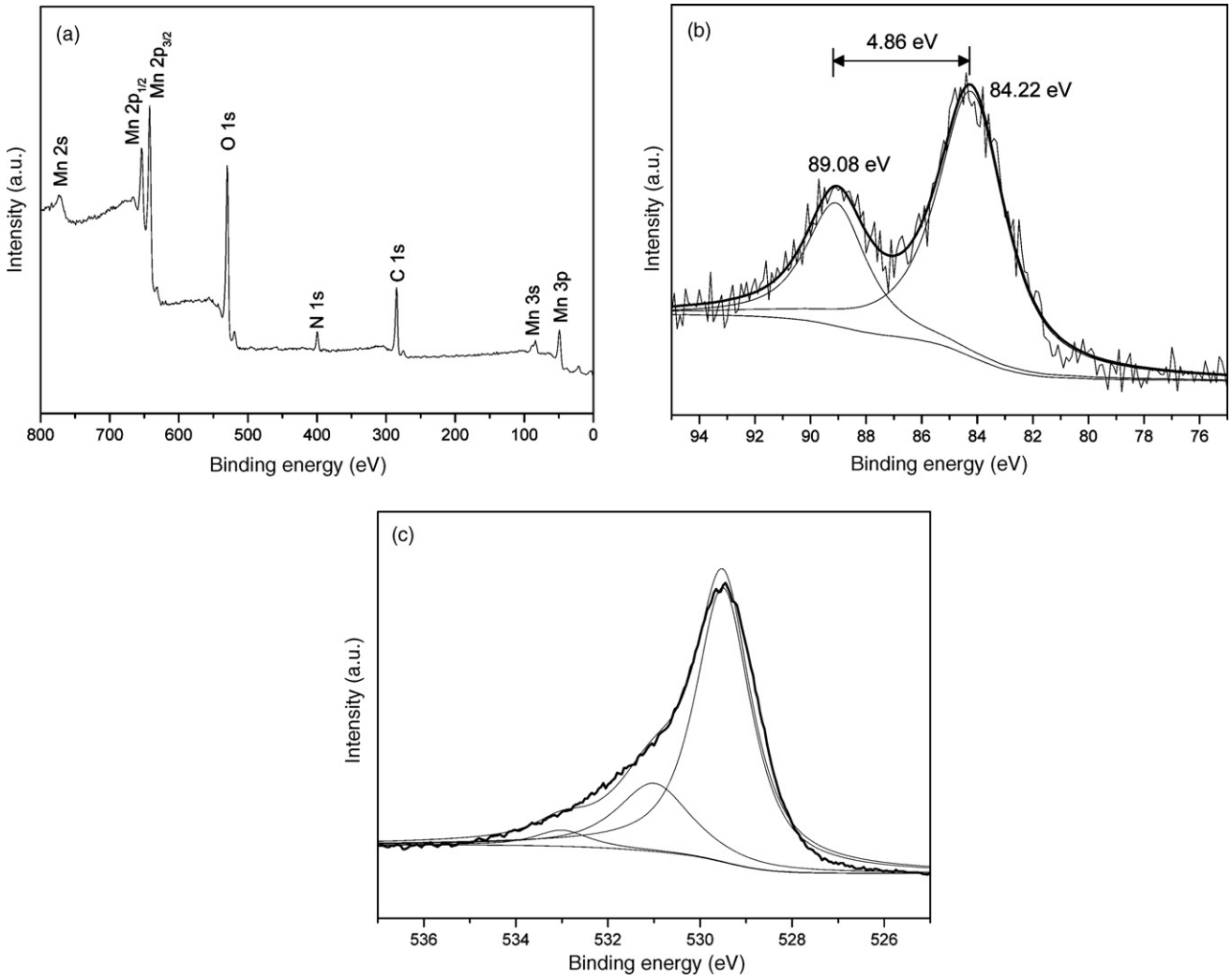

Fig. 3. XPS spectra for the film of $(PEI/MNS)_{10}$ prepared on quartz glass substrate: (a) survey spectrum, (b) Mn 3s and (c) O 1s region.

The Mn 2p region consists of a spin–orbit doublet with binding energy of 654.1 eV (Mn $2p_{1/2}$) and 642.1 eV (Mn $2p_{3/2}$), which are characteristics of a mixed-valence manganese system (Mn^{4+} and Mn^{3+}). In Fig. 3b, the Mn 3s core level spectrum exhibits multiple splitting in the form of two peaks at 89.08 and 84.22 eV. The separation of the peak energy (ΔE) is sensitive to the oxidation state of manganese. According to the linear relationship between the average oxidation state of manganese and the ΔE value in the literature [25], the ΔE value (4.86 eV) obtained corresponds to an average oxidation level of 3.7–3.8, which is typical of birnessite-type manganese oxide [26]. In the O 1s region (Fig. 3c), three different contributions are observed at 529.5, 531.0 and 533.0 eV, which can be assigned to oxide (Mn–O–Mn), hydroxide (Mn–OH), and structural water, respectively [27]. The average oxidation state of manganese can be determined from the O 1s core level spectrum [28], since the peak area contributions of the Mn–O–Mn and Mn–OH components are given by the following equation:

$$\text{oxidation state} = \frac{[\text{IV} \times (S_{\text{Mn-O-Mn}} - S_{\text{Mn-OH}}) + (\text{III} \times S_{\text{Mn-OH}})]}{S_{\text{Mn-O-Mn}}} \quad (1)$$

where S stands for the peak area contribution of each component of the O 1s spectrum. The average oxidation state of manganese obtained from Eq. (1) is 3.7 for the film, which is consistent with the value calculated above from the Mn 3s splitting. XPS quantitative analysis revealed that the atomic ratio of Mn to N is 3.0 for the film.

FESEM images of $(PEI/MNS)_{10}$ thin film on ITO-coated glass substrate are shown in Fig. 4. The film has a smooth and dense surface in the top view (Fig. 4a). The surface is covered with plate-like particles with lateral dimensions in the range from several tens to several hundreds of nanometers. Each MNS is glued together with the others by the polyelectrolyte layer deposited (Fig. 4b). This is similar to the case of the layered organic–inorganic composite films made from montmorillonite clay platelets and polyelectrolyte by the LBL technology [29]. The edge view image shows the film is uniform in thickness (Fig. 4c). A high magnification FESEM cross-section image of the film reveals a layered structure and the thickness of the film is about 200 nm. Such a special microstructure can improve the high-rate capability and the electrochemical stability of the electrode.

CV was used to investigate the capacitive behaviors of multilayer thin films. Fig. 5 shows the CV curves of the multilayer thin films of $(PEI/MNS)_1$, $(PEI/MNS)_5$, $(PEI/MNS)_{10}$ and $(PEI/MNS)_{15}$ at a scan rate of 10 mV s^{-1} in a 2 M KCl aqueous solution. All the CV curves of the films with different deposition layers show roughly rectangular mirror images with respect to the zero-current line, which indicate the capacitive behaviors. Fig. 6 shows the variation of the specific capacitance of $(PEI/MNS)_n$ multilayer thin films with the number of bilayers. The area specific capacitance values of $(PEI/MNS)_n$ multilayer

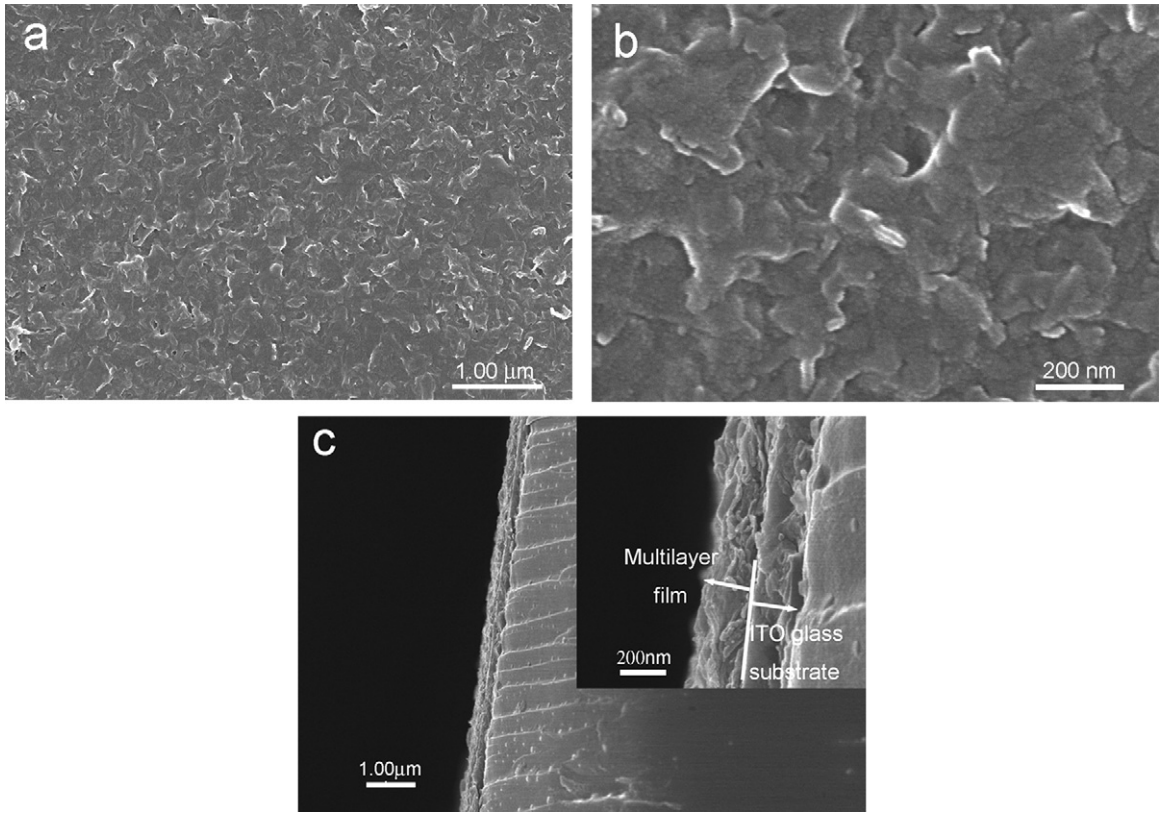

Fig. 4. FESEM images of $(PEI/MNS)_{10}$ film on ITO-coated glass substrate: (a) top view, (b) same as (a) at a high magnification and (c) edge view with a high-resolution image shown in the insert.

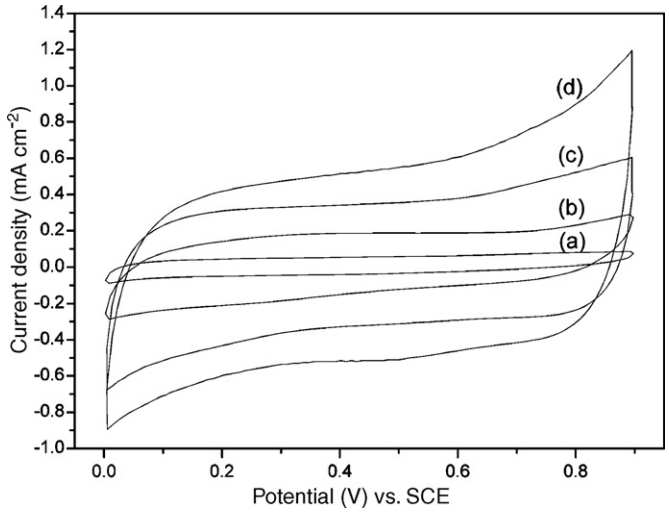

Fig. 5. Cyclic voltammograms of $(PEI/MNS)_n$ multilayer thin films on ITO-coated glass substrates: $n = 1, 5, 10, 15$ for a, b, c, d, respectively. The scan rate is 10 mV s^{-1}.

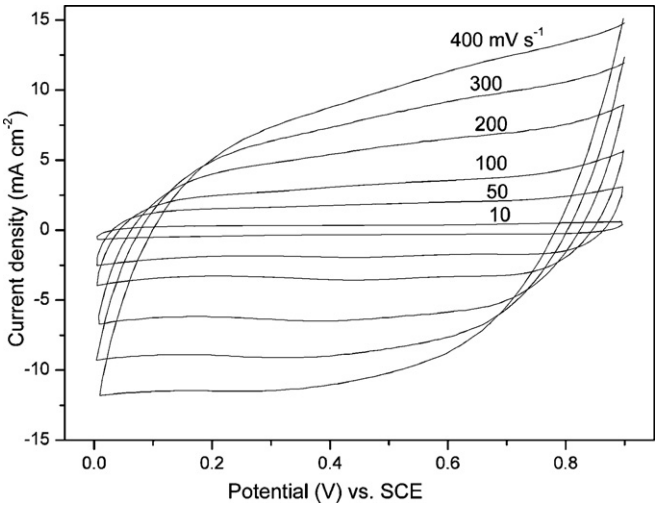

Fig. 7. Cyclic voltammograms of $(PEI/MNS)_{10}$ thin film on ITO-coated glass substrate at different potential scan rates.

thin films enhance almost linearly with an increase in the number of bilayers (within 15 bilayers), indicating that approximately equal amounts of electrochemically active manganese oxides are incorporated into the films for each deposition cycle.

Fig. 7 shows the CV curves of $(PEI/MNS)_{10}$ film at different scan rates of 400, 300, 200, 100, 50 and 10 mV s^{-1}. The shape of voltammetric curves is not significantly influenced by the scan rate of CV. The CV curves are rectangular and symmetrical even at very high scan rate of 400 mV s^{-1}. This result indicates that $(PEI/MNS)_{10}$ film shows excellent electrochemical activity, high reversibility and high power density.

Fig. 8 shows the charge–discharge behaviors of $(PEI/MNS)_{10}$ film at different current densities. The charge curves are very symmetric to the corresponding discharge counterparts in the whole potential region, and the slopes of curves are potential independent and maintain the constant values. The result also indicates the $(PEI/MNS)_{10}$ film has the ideal capacitive behavior for supercapacitors. The deposited manganese oxide of the $(PEI/MNS)_{10}$ film was 20 ± 1 μg cm^{-2}, which was obtained by the ICP measure. So, the specific capacitance values are 210, 240, 265 and 288 F g^{-1} for the current densities of 12.5, 5, 2.5 and 1.25 A g^{-1}, respectively. The capacitance retention is about 73%, with growth of current densities from 1.25 to 12.5 A g^{-1}.

Fig. 9 shows the charge–discharge cycling test of $(PEI/MNS)_{10}$ film at a high current density of 2.5 A g^{-1} between 0 and 0.9 V versus SCE. After 1000 cycles of operation, the capacitance decreases 9.5% of initial capacitance. The decrease of specific capacitance could be attributed to the partial dissolution of manganese oxide from the $(PEI/MNS)_{10}$ film into the electrolytes during cycling [5].

As observed from the CV and constant current charge–discharge curves, the $(PEI/MNS)_n$ multilayer thin films show good electrochemical properties, which can be attributed to the fact that MNS being a semiconductor, thin films therefore possess considerable lower resistivity for electron

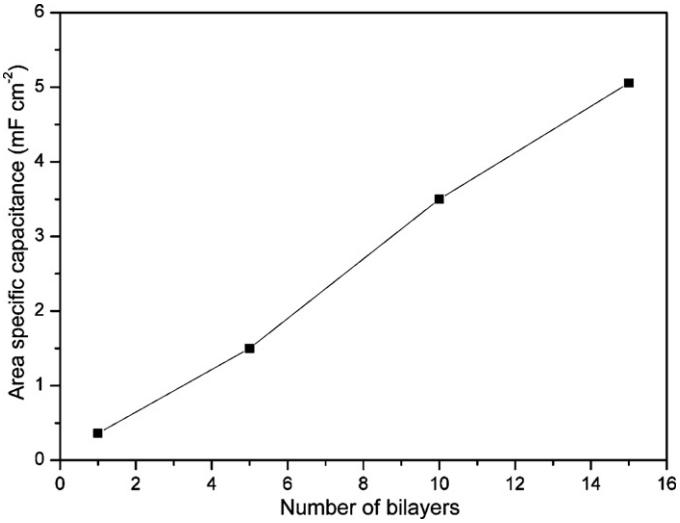

Fig. 6. The dependence of the area specific capacitance on the number of bilayers.

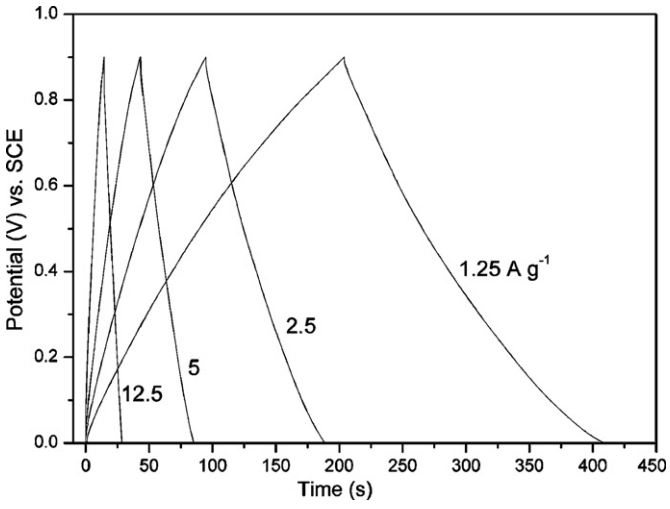

Fig. 8. Galvanostatic charge–discharge curves of $(PEI/MNS)_{10}$ thin film on ITO-coated glass substrate at different current densities.

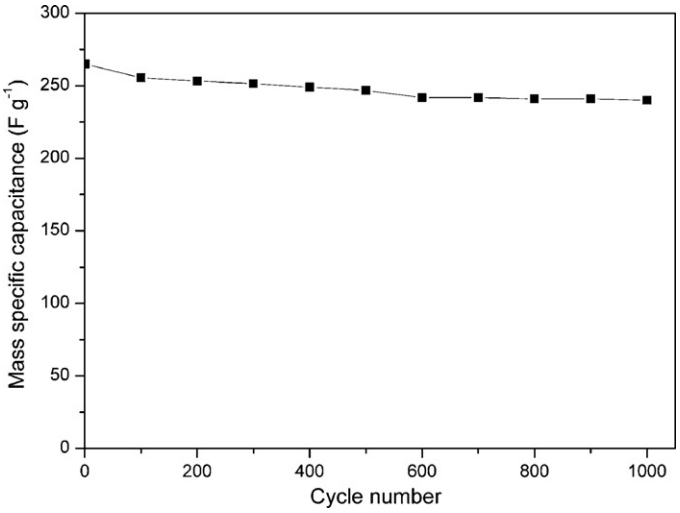

Fig. 9. Cyclic performance of $(PEI/MNS)_{10}$ thin film on ITO-coated glass substrate at a current density of 2.5 A g^{-1}.

conduction across the film matrix onto the current collector. The nanoscale thickness of nanosheets also provides a shorter diffusion path length, with enhanced proton diffusion kinetics into and out of bulk materials. Moreover, polyethylenimine polyelectrolyte as binder enables the formation of adherent films to the substrates, which can improve the electrochemical stability of the electrodes.

4. Conclusion

In summary, we demonstrated the fabrication of multilayer thin films via LBL self-assembly of MNS and polyethylenimine polyelectrolyte. UV–vis absorption spectra showed that approximately equal amounts of manganese oxides were incorporated into the films for each deposition cycle. The multilayer thin film showed a good electrochemical performance, which could be attributed to the special microstructure of the film electrode. The specific capacitance value of 288 F g^{-1} for $(PEI/MNS)_{10}$ film on ITO-coated substrate was obtained at the current density of 1.25 A g^{-1}. The LBL self-assembly technology provided a simple and effective method for preparing thin film electrodes for electrochemical capacitors.

Acknowledgements

We would like to thank the National Natural Science Foundation of China (Grant No. 20301002), the National 863 Project (Grant No. 2006AA03Z343), the 111 Project (Grant No. B07004), and Program for Changjiang Scholars and Innovative Research Team in University (Grant No. IRT0406) for financial support.

References

[1] A. Burke, J. Power Sources 91 (2000) 37.
[2] M. Winter, R.J. Brodd, Chem. Rev. 104 (2004) 4245.
[3] A.S. Arico, P. Bruce, B. Scrosati, J.-M. Tarascon, W.V. Schalkwijk, Nat. Mater. 4 (2005) 366.
[4] J.P. Zheng, P.J. Cygan, T.R. Jow, J. Electrochem. Soc. 142 (1995) 2699.
[5] S.-C. Pang, M.A. Anderson, T.W. Chapman, J. Electrochem. Soc. 147 (2000) 444.
[6] S.-C. Pang, M.A. Anderson, J. Mater. Res. 15 (2000) 2096.
[7] S.-F. Chin, S.-C. Pang, M.A. Anderson, J. Electrochem. Soc. 149 (2002) A379.
[8] J.-K. Chang, W.-T. Tsai, J. Electrochem. Soc. 150 (2003) A1333.
[9] M. Nakayama, A. Tanaka, Y. Sato, T. Tonosaki, K. Ogura, Langmuir 21 (2005) 5907.
[10] N. Nagarajan, H. Humadi, I. Zhitomirsky, Electrochim. Acta 51 (2006) 3039.
[11] T. Xue, C.-L. Xu, D.-D. Zhao, X.-H. Li, H.-L. Li, J. Power Sources 164 (2007) 953.
[12] M. Nakayama, T. Kanaya, R. Inoue, Electrochem. Commun. 9 (2007) 1154.
[13] Y. Dai, K. Wang, J. Zhao, J. Xie, J. Power Sources 161 (2006) 737.
[14] K.-W. Nam, K.-B. Kim, J. Electrochem. Soc. 153 (2006) A81.
[15] J.N. Broughton, M.J. Brett, Electrochim. Acta 49 (2004) 4439.
[16] B. Djurfors, J.N. Broughton, M.J. Brett, D.G. Ivey, J. Power Sources 156 (2006) 741.
[17] B. Djurfors, J.N. Broughton, M.J. Brett, D.G. Ivey, J. Electrochem. Soc. 153 (2006) A64.
[18] L. Wang, Y. Omomo, N. Sakai, K. Fukuda, I. Nakai, Y. Ebina, K. Takada, M. Watanabe, T. Sasaki, Chem. Mater. 15 (2003) 2873.
[19] L. Wang, N. Sakai, Y. Ebina, K. Takada, T. Sasaki, Chem. Mater. 17 (2005) 1352.
[20] R. Kniprath, S. Duhm, H. Glowatzki, N. Koch, S. Rogaschewshi, J.P. Rabe, S. Kirstein, Langmuir 23 (2007) 9860.
[21] W. Sugimoto, H. Iwata, Y. Yasunaga, Y. Murakami, Y. Takasu, Angew. Chem. Int. Ed. 42 (2003) 4092.
[22] Y. Wang, W. Yang, J. Yang, Electrochem. Solid-State Lett. 10 (2007) A233.
[23] Z. Liu, K. Ooi, H. Kanoh, W. Tang, T. Tomida, Langmuir 16 (2000) 4154.
[24] Y. Omomo, T. Sasaki, L. Wang, M. Watanabe, J. Am. Chem. Soc. 125 (2003) 3568.
[25] M. Toupin, T. Brousse, D. Belanger, Chem. Mater. 14 (2002) 3946.
[26] M. Nakayama, M. Fukuda, S. Konishi, T. Tonosaki, J. Mater. Res. 21 (2006) 3152.
[27] M. Chigane, M. Ishikawa, J. Electrochem. Soc. 147 (2000) 2246.
[28] M. Toupin, T. Brousse, D. Belanger, Chem. Mater. 16 (2004) 3184.
[29] Z. Tang, N.A. Kotov, S. Magonov, B. Ozturk, Nat. Mater. 2 (2003) 413.